Theor Chem Acc (2007) 118:185–191
DOI 10.1007/s00214-007-0273-y

REGULAR ARTICLE

Effects of water re-location and cavity trimming on the CASPT2//CASSCF/AMBER excitation energy of Rhodopsin

Angela Strambi · Pedro B. Coto · Nicolas Ferré · Massimo Olivucci

Received: 18 December 2006 / Accepted: 22 February 2007 / Published online: 28 March 2007

Abstract We have used quantum-mechanics/molecular-mechanics computations based on *ab initio* multiconfigurational perturbation theory to determine and rationalize the effect of the re-location of one crystallographic water molecule on the vertical excitation energy of the visual pigment rhodopsin. It is found that the re-location of one water molecule to the opposite side of the 11-*cis* retinal chromophore leads to a large 0.7–0.8 Å contraction in the chromophore—counterion salt-bridge distance. In spite of this structural effect, the change in excitation energy is found to be limited (< 1.5 kcal mol^{-1}). Through an analysis of different rhodopsin models in terms of "components" (isolated chromophore, isolated chromophore—counterion ion-pair and models deprived of the counterion charges) we show that the limited change of the excitation energy can be related to a displacement of the retinal chromophore to a different spot of the protein cavity.

Contribution to the Fernando Bernardi Memorial Issue.

A. Strambi · P. B. Coto · M. Olivucci
Dipartimento di Chimica, Università di Siena, via Aldo Moro 2, 53100 Siena, Italy

N. Ferré
Laboratoire de Chimie Théorique et de Modélisation Moléculaire, UMR 6517- CNRS Université de Provence, Case 521, Faculté de Saint-Jérôme, Av. Esc. Normandie Niemen, 13397 Marseille Cedex 20, France

M. Olivucci (✉)
Chemistry Department, Bowling Green State University, Bowling Green, OH 43403, USA
e-mail: olivucci@unisi.it; molivuc@bgsu.edu

1 Introduction

Recently, we have shown that "brute force" quantum-mechanics/molecular-mechanics (QM/MM) computations based on ab initio (i.e., first principles) multiconfigurational perturbation theory can reproduce the absorption maxima of a set of modified rhodopsins with an accuracy allowing for the analysis of the factors determining their colors [1]. In particular, for rhodopsin itself (the visual pigment of superior animals) the computed vertical excitation energies (478 and 327 nm) [2] from the ground state to the first singlet excited state ($S_0 \rightarrow S_1$) and from the ground state to the second singlet excited state ($S_0 \rightarrow S_2$) are only 3 kcal mol^{-1} off the experimentally observed λ^a_{max} value (498 and 340 nm) [3], the computed 14.6 D $S_0 \rightarrow S_1$ change in dipole moment ($\Delta\mu$) falls within the observed 13–15 D range [4] and the $S_0 \rightarrow S_1$ f value (0.8) compares well with the experimental quantity (1.0) [3].

The results above are relative to a computational model of bovine rhodopsin (*Rh*) derived from monomer A deposited in the PDB archive as file 1HZX [5]. In such model the crystallographic structure, resolved at 2.8 Å, is assumed to provide an acceptable model of the average environment of the chromophore. Accordingly, no protein solvent (membrane lipids and external waters) is added. Furthermore, two internal water molecules have been introduced in the model. The first one, present in the crystal structure, is located between the protein 11-*cis* retinal chromophore (PSB11) and Glu181 residue. A second one (see Fig. 1) has been placed between PSB11 (a protonated Schiff base cation) and its Glu113 carboxyl counterion, as suggested by Kandori et al. [6].

Recently, two better resolved crystallographic structures (1L9H at 2.6 Å and 1U19 at 2.2 Å in the PDB archive) [7,8] reporting the position of the W2 water have become available. Such a position differs significantly from that defined in

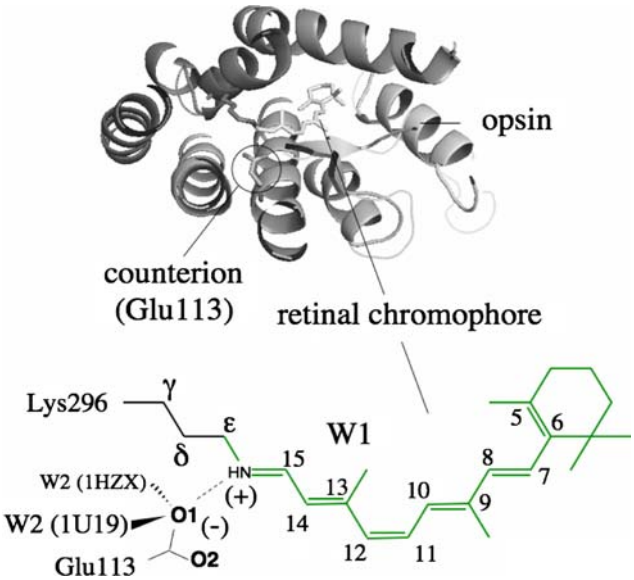

Fig. 1 *Top* view of rhodopsin from the cytoplasmatic side. *Bottom* schematic structure of the 11-*cis* retinal chromophore. Notice the different position of the W2 water in the alternative 1HZX (*Rh* model) and 1U19 (*Rh-1U19* model) structures

our original model. Indeed, as schematically shown in Fig. 1, while W2 is invariably hydrogen bonded to O1 (i.e., to the Glu113 carboxylate), its position is shifted to the opposite side of the rhodopsin 11-*cis* retinal chromophore (PSB11). The fact that *Rh* reproduces the observed $\lambda^a_{\max}$ values of rhodopsin and yet presents a W2 position not consistent with the best available crystallographic data opens the question of the sensitivity of the spectral parameters to internal water re-location. Thus, in this contribution we report a quantitative investigation of the changes in excitation energy produced by a re-location of W2 in the counterion region. This is carried out looking at a new model based on the 1U19 structure (*Rh-1U19*). The results show that, in spite of significant geometry changes in the Schiff base region, the re-computed excitation energy differs less than 1 kcal mol^{-1} from the original value. It is also shown that an analysis of the excitation energies of the PSB11—Glu113 ion-pairs, extracted by *Rh* and *Rh-1U19* structures, indicates that PSB11 is re-located inside the protein cavity in such a way to counterbalance the electrostatic effect of the contraction of the NH(+)—O1(−) salt-bridge distance.

An additional result reported below attempts to provide an answer to the question of determining which portion of the chromophore environment in the *Rh* model is held responsible for the excitation energy value. It is shown that, within our QM/MM treatment, a reduced opsin model incorporating only the residues surrounding the chromophore — i.e., the so called Palczewski's cavity [5]—yields an excitation energy value close to those computed for the full opsin.

2 Models and methods

The (original) *Rh* model considered in this work is derived from monomer A deposited in the PDB archive as file 1HZX [5]. With the exception of Lys296, the residue charges are described by the standard AMBER force field [9] and thus the residue polarizability or/and dispersion effects are not explicitly treated. As originally pointed out by Warshel [10,11], a correct model should include the protein solvent and account for the solvent and protein polarizability. On the other hand, the effect of the residue polarizability and dispersion on the absolute excitation energy has been shown to be limited (for the related protein bacteriorhodopsin Warshel et al. estimated [12] an effect of <1,500 cm^{-1} . See also the work by Ren et al. [13], Matsuura et al. [14] and Rajamani et al. [15]) and shall fall into the reported blue-shifted and 4.5 kcal mol^{-1} error (notice that cancellation effects cannot be excluded). With the exception of the Glu113 counterion [forming a salt-bridge with NH(+)] the model cavity is set neutral consistently with the experiment [16]. While the protein backbone and residues are kept frozen during the optimization, the Lys296 side chain, the position/orientation of two TIP3P water molecules [W1 and W2(1HZX) in Fig. 1] and the chromophore are relaxed to generate the protein equilibrium structure. The optimization has been stopped when the maximum force is <0.0015 hartree/bohr and the rms is <0.001 bohr (Due to the excessive computational cost no second derivative computation could be performed to rigorously determine the nature of the stationary point). The alternative *Rh-W2-NewPos* model is a modification of the above model where the W2 water has been moved to the opposite side of the retinal consistently with the 1U19 crystallographic structure and re-optimized according to the same procedure. However, notice that in this model the protein cavity correspond to that of the 1HZX structure. Finally, model *Rh-1U19* is a model produced with the same procedure used for *Rh* but where the initial crystallographic structure corresponds to 1U19 and comprises the two resolved waters W1 and W2 (i.e., W1 and W2(1U19) in Fig. 1).

The QM/MM scheme used to evaluate (when appropriate) the model equilibrium structures and related spectral parameters is fully described in ref. [17]. Briefly, the method is based on a hydrogen link-atom scheme [18] with the frontier placed at the C_δ–C_ε bond of the Lys296 side chain (see Fig. 1). The *ab initio* QM calculations are based on a CASSCF/6-31G* level. The active space comprises the full π-system of PSB11 (12 electrons in 12 π-orbitals). The MM (we use the AMBER force field) and QM segments interact in the following way: (i) all QM atoms feel the electrostatic potential of the MM point charges, (ii) stretching, bending and torsional potentials involving at least one MM atom are described by the MM potential (iii) QM and MM atom pairs separated by more then two bonds interact via either standard

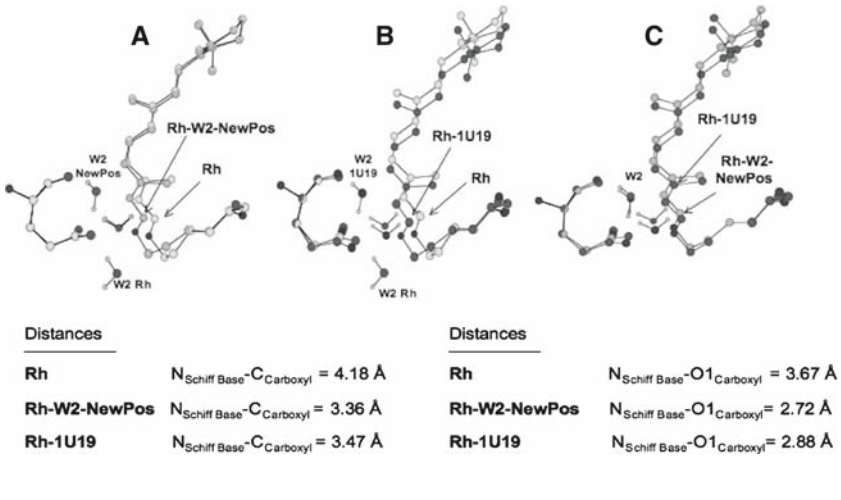

Fig. 2 **A** Superposition of the optimized S_0-*Rh* (*white*) and S_0-*Rh-W2-NewPos* (*gray*) retinal chromophores. **B** Superposition of the optimized S_0-*Rh* (*white*) and S_0-*Rh-1U19* (*black*) retinal chromophores. **C** Superposition of the optimized S_0-*Rh-W2-NewPos* (*gray*) and S_0-*Rh-1U19* (*black*) retinal chromophores. *Bottom* distances between the nitrogen of the protonated Schiff base and the carbon of the carboxylic group of the Glu113 counterion and between the same nitrogen and the O1 of the carboxylic group of Glu113 counterion

or re-parametrized ([19,20]) van der Waals potentials. CASSCF/6-31G*/AMBER geometry optimization is carried out with the GAUSSIAN03 [21] and TINKER [22] programs. The ultimate goal was to obtain $\lambda^a_{\max}$ and oscillator strengths for S_0->S_1 and S_0->S_2 transitions of PSB11 in the environment of the defined protein models.

3 Results and discussion

In order to estimate the influence of the (i) position of the internal water W2 and (ii) reduction of the protein (i.e., opsin) model on the CASPT2//CASSCF/6-31G*/AMBER spectral parameters of rhodopsin we consider six models. These include the *Rh*, *Rh-W2-NewPos* and *Rh-1U19* models defined in Sect. 2 and featuring a complete opsin environment and the *Rh-Cavity*, *Rh-W2-NewPos-Cavity*, *Rh-1U19-Cavity* models derived from the previous set through a drastic reduction of the opsin models. More specifically, the reduced models contain exclusively the 27 residues surrounding the chromophore and defining the Palczewski's cavity (see above). Notice that these trimmed models are exclusively used for re-evaluation of the excitation energy and thus the structure is not re-optimized.

3.1 Effects of the position of W2

The ground state equilibrium structures of the retinal chromophore of models *Rh-W2-NewPos* and *Rh-1U19* are reported in Fig. 2. The superposition with *Rh* reveals that the W2 re-location leads to a large 0.7–0.8 Å contraction of the distance between the nitrogen of the Schiff base group and the Glu113 carboxylate. Furthermore (see also Fig. 3), in both *Rh-W2-NewPos* and *Rh-1U19*, the W2 water molecule forms two hydrogen bonds involving the O1 oxygen of the counterion and the carbonyl oxygen of the nearby peptide bond, respectively. Such hydrogen bonded structure must lead to

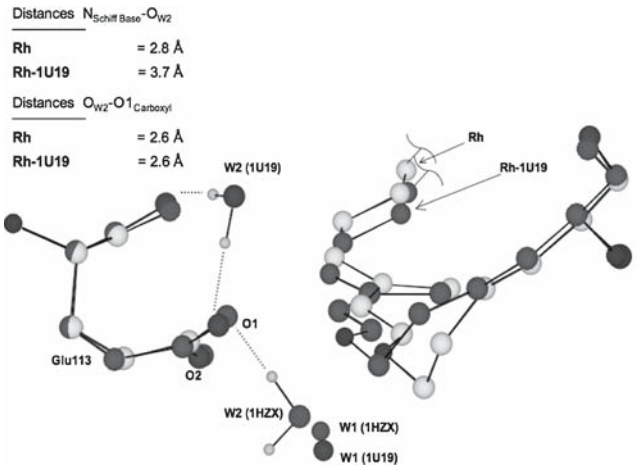

Fig. 3 Superposition of the optimized S_0-*Rh* (*white*) and S_0-*Rh-1U19* retinal chromophores (*black*). Some critical distances describing the position of the W2 water are reported. Notice that the position/orientation of *W2* for *Rh-W2-NewPos* is very similar to that one of *Rh-1U19* model

a significant stabilization of the W2 position consistently with the fact that the original *Rh* model, where W2 is hydrogen bonded to a single carboxylate oxygen, is 17 kcal mol^{-1} higher in energy with respect to *Rh-W2-NewPos*. This type of binding is also found in the *1U19* crystallographic structure as well as in previously reported DFT-based models [23,24].

The superposition of the three models (see Fig. 2) reveals an important re-location of the retinal chromophore dominated by the displacement of the Schiff base region. However, it must be stressed that, in both *Rh-W2-NewPos* and *Rh-1U19*, the PSB11 optimized geometry is quite similar, in terms of dihedral angles, to the PSB11 geometry reported for the original *Rh* model (see Table 1). (It may be noticed that, in *Rh-1U19*,the PSB11 backbone becomes fairly more planar). The computed displacement is very similar in the *Rh-W2-NewPos* and *Rh-1U19* geometries. These results also show that the position of W1 is little affected by the re-location of W2.

Table 1 Dihedral angles (degrees) along the backbone of the 11-*cis* retinal chromophore

Model	$C_6 = C_7$	$C_7 = C_8$	$C_8 = C_9$	$C_9 = C_{10}$	$C_{10} = C_{11}$	$C_{11} = C_{12}$	$C_{12} = C_{13}$	$C_{13} = C_{14}$	$C_{14} = C_{15}$	$C_{15} = N_{16}$
Rh	−54.0°	175.9°	−170.2°	169.7°	166.1°	−8.1°	166.6°	178.9°	177.7°	173.2°
Rh-W2-NewPos	−55.4°	175.1°	−170.0°	167.0°	175.1°	−7.8°	166.7°	177.9°	172.8°	171.4°
Rh-1U19	−53.2°	−177.9°	−172.6°	174.0°	170.9°	−4.0°	165.4°	−179.2°	169.6°	171.9°

Notice that $C_6 = C_7$ defines the dihedral angle of the β-ionone ring while $C_{11} = C_{12}$ corresponds to the dihedral angle of the isomerizing double bond

Table 2 Calculated and observed λ^a_{max} values (nm)

Structure	Calculated	Observed	Error
	λ^a_{max}	λ^a_{max}	
S_0-*Rh*	478 (59.83)	498 (57.4)	< 2.5
S_0-*Rh-W2-NewPos*	479 (59.77)		< 2.5
S_0-*Rh-1U*19	513 (55.74)		> −1.8

Excitation energies (kcal mol^{-1}) are given in parenthesis. The upper limit of the error computed with respect to the observed λ^a_{max} value, is given in kcal mol^{-1}

The $S_0 \rightarrow S_1$ excitation energies and corresponding λ^a_{max} values for our three rhodopsin models are reported in Table 2. The absolute error, with respect to the experiment, is also reported. In spite of the fact that the structural changes described above must strongly modify the chromophore-counterion electrostatic interaction, the computed excitation energies are similar. In fact, the predicted energy is always less than 3 kcal mol^{-1} far from the experimental value, even if for *Rh-1U19* the error yields a red shifted rather than a blue shifted predicted value. The electrostatic interactions are considered one of the most important factors affecting the value of the spectral parameters in rhodopsin. Hence, given the remarkable change in NH(+)—O1(−) salt bridge distance between *Rh* and models *Rh-W2-NewPos* and *Rh-1U19*, a significant change in excitation energy was expected. Indeed, it is established [25] that the shorter is the distance between the negatively charged counterion and the positive Schiff base group, the larger is the stabilization of the ground state with respect to the spectroscopic state ultimately leading to a blue-shift in the chromophore absorption.

This behavior is readily explained by the charge-transfer nature of the spectroscopic state of the chromophore [4,26–28]. In fact, upon vertical $S_0 \rightarrow S_1$ transition, the chromophore positive charge, located initially on the –NH=CH– moiety, shifts towards the β-ionone region leading to counterion—chromophore charge separation. As a consequence, any electrostatic effect that stabilizes (destabilizes) the positive charge in the Schiff base region on the ground state, as well as any electrostatic effect that destabilizes (stabilizes) the positive charge in the proximity of β-ionone region will lead to an augmented (reduced) $S_0 \rightarrow S_1$ energy gap. For this reason it is rather surprising that models *Rh-W2-NewPos* and the *Rh-1U19* do not show a large blue-shift in excitation energy with respect to *Rh*.

In order to rationalize the behavior described above, we have "dissected" the excitation energies of the three models (see Fig. 4). More specifically we have determined, for each model and using the same level of theory, the excitation energies of (i) the full protein, (ii) the isolated chromophore (taken with the geometry found in the protein), (iii) the chromophore-Glu113 ion pair (also taken with the geometry found in the protein) and (iv) the full protein model deprived of the Glu113 counterion charges (this is called non-counterion-opsin (nc-opsin) from now on). From the values of the excitation energies of the isolated chromophores (see Fig. 4B) it is apparent that the limited differences in the retinal structure have a small effect on the excitation energy values. In contrast, due to the difference in $N_{Schiff\ base}$–$C_{Carboxyl}$ values (see Fig. 2), a substantial difference is expected for the excitation energy of the chromophore-Glu113 ion-pairs. In fact, the ion-pairs extracted from the *Rh-W2-NewPos* and *Rh-1U19* models give blue-shifted values with respect to the corresponding *Rh* ion-pair (see Fig. 4C), reflecting the stronger electrostatic interaction of the negative counterion with the positive chromophore.

The fact that, in contrast to the isolated ion-pair, the excitation energy of *Rh* (see Fig. 4A) is closer to those of *Rh-W2-NewPos* and *Rh-1U19*, must be attributed to the effect of the cavity residues other than the Glu113 counterion. This conclusion is confirmed by the data reported in Fig. 4D where we show the effect of the nc-opsin cavity (i.e., a cavity with a neglected counterion charge). It is apparent by inspection of the figure that the excitation energies are all red-shifted with respect to those of the isolated chromophores (as previously reported [1] this counterbalance, to some extent, the effect of the counterion that always leads to a blue-shift). Secondly, the excitation energy of *Rh* is the least red-shifted. In other words, while the nc-opsin cavity of the *Rh-W2-NewPos* and *Rh-1U19* models strongly red-shifts the chromophore absorption, such an effect is more limited in *Rh*. Remarkably, this lesser effective red-shift appears to match and counterbalance the lesser effective blue-shift seen in the ion-pair and due to the larger distance between the counterion and Schiff base charges.

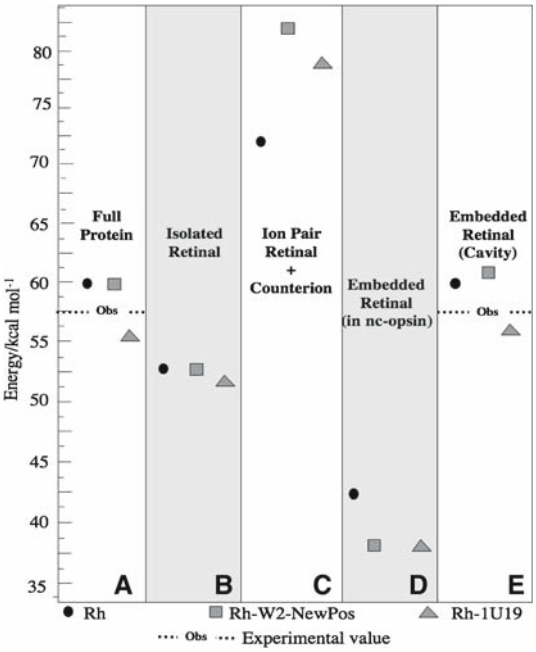

Fig. 4 Excitation energies analysis for *Rh*, *Rh-W2-NewPos* and *Rh-1U19*. **A** Full rhodopsin model. **B** Isolated retinal chromophore. **C** Isolated chromophore-counterion pair. **D** Chromophore embedded in an artificial opsin (nc-opsin) deprived of the counterion charges. **E** Rhodopsin models with a trimmed opsin (*Rh-Cavity*, *Rh-W2-NewPos-Cavity* and *Rh-1U19-Cavity*)

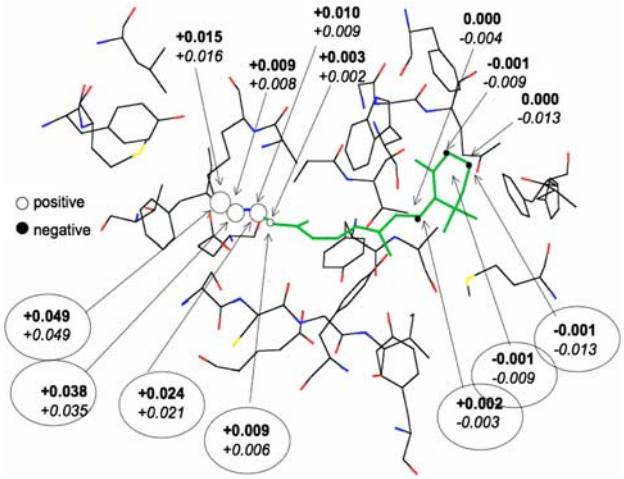

Fig. 5 Change in the electrostatic potential generated by the AMBER partial charges of nc-opsin on the atoms of the retinal chromophore of *Rh-W2-NewPos* (*bold*) and *Rh-1U19* (*italics*) with respect to the same potential calculated for the reference *Rh* model. Noticed that, in the protonated Schiff base region, the nc-opsin potential is always positive. Circled values report the variations, again with respect to *Rh*, when W1 and W2 are included in the computation (i.e., when the electrostatic potential is generated by nc-opsin + W1 + W2)

While the reason for a less effective blue-shift in the *Rh* ion-pair can be safely attributed to the larger distance between the Glu113 carboxylate and Schiff base group of this model, the reason for the less effective red-shift induced by nc-opsin cannot be immediately understood. This effect must be obviously related to the structure and intensity of the electric field, generated by the partial charges of the neutral protein residues, acting on the chromophore nuclei. For *Rh* we found a positive potential in the Schiff base region [1] destabilizing S_0 with respect to S_1 (see above). Here, we report that such potential increases in intensity for *Rh-W2-NewPos* and *Rh-1U19* consistently with the stronger red-shift seen in Fig. 4D. This is documented in Fig. 5 where we report the most significant differences between the nc-opsin potential of *Rh-W2-NewPos* and *Rh-1U19* with respect to the one calculated for *Rh*. Indeed, there is a remarkable ca. +0.15 a.u. increase in the Schiff base region due to the nc-opsin residues. We also show that the positive potential increase is enhanced when W2 is inserted in the nc-opsin model.

As previously reported [1], in our CASPT2//CASSCF/6-31G*/AMBER models, the negative counterion counterbalances and surmounts the nc-opsin potential thus accounting for the blue-shift imposed by the full protein on the excitation energy of the isolated chromophore. It is apparent from the data above, that the stronger (counterion-induced) blue-shift expected for *Rh-W2-NewPos* and *Rh-1U19* is counterbalanced by a stronger red-shift due to nc-opsin. However, notice that the nc-opsins in *Rh* and in *Rh-W2-NewPos* are *identical* as the cavity is derived by the same 1HZX crystallographic structure. The solution of this apparent discrepancy lies in the different orientation/placement of the retinal chromophore (especially of its Schiff base region). In fact, as seen in Fig. 2A, the re-location of the *Rh-W2-NewPos* chromophore relative to the *Rh* chromophore, leads to exposure to a different electrostatic potential. Our results suggest that the limited sensitivity of the computed excitation energy to W2 re-location is associated with a mechanism that re-locates the chromophore. This mechanism will be the subject of further investigations.

3.2 Reduction of the protein model

In this section we discuss the CASPT2//CASSCF/6-31G*/AMBER vertical excitation energies computed for the three trimmed rhodopsin models defined in Sect. 3. Our target is to assess whether the effect of the protein cavity on the chromophore λ^a_{max} is mainly due to the first shell of residues or to a more extensive portion of opsin. The results of these computations are reported in Tables 3 and 4. The differences between the excitation energies of the full models and of the corresponding trimmed models are < 1.5 kcal mol^{-1} for both the $S_0 \rightarrow S_1$ and $S_0 \rightarrow S_2$ transitions. Such a limited change indicates that, within our QM/MM protocol, the spectral properties of the chromophore are determined by the Palczewski's cavity. This conclusion may not hold if one

Table 3 Three-roots state average (equal weights) CASSCF/6-31G*/Amber and CASPT2/6-31G*/Amber excitation energies computed for $S_0 \rightarrow S_1$ and $S_0 \rightarrow S_2$ transitions in the full models and in the reduced ones expressed in kcal mol^{-1}

	S_1		S_2	
Structure	CASSCF	CASPT2	CASSCF	CASPT2
S_0-*Rh*	92.16	59.83	109.40	87.27
S_0-*Rh-W2-NewPos*	91.17	59.77	106.26	84.09
S_0-*Rh-1U19*	85.35	55.74	103.70	84.07
S_0-*Rh-Cavity*	93.20	59.77	110.41	86.88
S_0-*Rh-W2-NewPos-Cavity*	93.33	61.16	108.00	83.00
S_0-*Rh-1U19-Cavity*	87.63	55.89	104.97	83.89

Table 4 Charge transfer (Δq) (i.e., change in the positive charge of the –NH=C15– fragment), change in dipole moment ($|\Delta\mu|$) and change in Oscillator strenghts (f) computed at three-roots state average (equal weights) CASSCF/6-31G*/Amber

	Δq[a]		$\lvert\Delta\mu\rvert(Debye)$[b]		f[c]	
Structure	$S_0 \rightarrow S_1$	$S_0 \rightarrow S_2$	$S_0 \rightarrow S_1$	$S_0 \rightarrow S_2$	$S_0 \rightarrow S_1$	$S_0 \rightarrow S_2$
S_0-*Rh*	−0.3446	−0.1546	14.59	5.40	0.773	0.506
S_0-*Rh-W2-NewPos*	−0.3093	−0.1721	13.88	6.13	0.757	0.576
S_0-*Rh-1U19*	−0.3692	−0.1261	15.97	5.03	0.928	0.416
S_0-*Rh-Cavity*	−0.3362	−0.1778	14.50	6.09	0.702	0.565
S_0-*Rh-W2-NewPos-Cavity*	−0.2761	−0.2163	12.82	7.57	0.629	0.697
S_0-*Rh-1U19-Cavity*	−0.3575	−0.1533	15.79	5.76	0.830	0.493

[a] evaluated with Mulliken charges at CASSCF level

[b,c] evaluated at CASSCF level

attempts a geometry optimization where the Van der Waals forces play an important role. It is also remarkable that the computed electronic structure properties (see Table 4) also remain qualitatively consistent in the three models, although larger differences are computed for *Rh-W2-NewPos*.

4 Conclusions

The sensitivity of *ab initio* CASPT2//CASSCF $S_0 \rightarrow S_1$ excitation energies to the position of the crystallographic water W2 has been assessed for different models of bovine rhodopsin. The results indicate a fairly low sensitivity of the absorption maximum to the W2 position that, in turn, suggests a compensation mechanism. Our analysis points to a displacement of the chromophore to a cavity region with a larger nc-opsin positive potential as a means to offset the effect of the decrease in NH(+)—O1(−) salt bridge distance. We have also compared the effect of a reduction of the full opsin model to the 27 aminoacids of the Palczewski's cavity. The fact that the value predicted for the $S_0 \rightarrow S_1$ excitation energy is substantially the same indicates that, for rhodopsin, the charges of distant residues are of relatively minor importance for the control of the optical absorption features of the retinal chromophore. Of course, we do not expect this to be a general result and highly truncated protein models should always be applied carefully until a systematic analysis is carried out to set their limitations and reliability.

References

1. Coto PB, Strambi A, Ferré N, Olivucci M (2006) Proc Natl Acad Sci USA 103:17154–17159
2. Andruniów T, Ferré N, Olivucci M (2004) Proc Natl Acad Sci USA 101:17908–17913
3. Hurley JB, Ebrey TG, Honig B, Ottolenghi M (1977) Nature 270:540–542
4. Mathies RA, Stryer L (1976) Proc Nat Acad Sci USA 73:2169–2173
5. Teller DC, Okada T, Behnke CA, Palczewski K, Stenkamp RE (2001) Biochemistry 40:7761–7772
6. Kandori H, Schichida Y, Yoshisawa T (2001) Biochemistry (Moscow) 66:1197–1209
7. Okada T, Fujiyoshi Y, Silow M, Navarro J, Landau EM, Shichida Y (2002) Proc Natl Acad Sci USA 99:5982–5987
8. Okada T, Sugihara M, Bondar AN, Elstner M, Entel P, Buss V (2004) J Mol Biol 342:571–583
9. Cornell WD, Cieplak P, Bayly CI, Gould IR, Jr KMM, Ferguson DM, Spellmeyer DC, Fox T, Caldwell JW, Kollman PA (1995) J Am Chem Soc 117:5179–5197
10. Warshel A (1976) Nature (London) 260:679–683
11. Warshel A, Chu ZT, Hwang J-K (1991) Chem Phys 158:303–314
12. Warshel A, Chu ZT (2001) J Phys Chem B 105:9857–9871

13. Ren L, Martin CH, Wise KJ, Gillespie NB, Luecke H, Lanyi J, Spudich JL, Birge RR (2001) Biochemistry 40:13906–13914
14. Matsuura A, Sato H, Houjou H, Saito S, Hayashi T, Sakurai M (2006) J Comp Chem 27:1623–1630
15. Rajamani R, Gao J (2002) J Comp Chem 23:96–105
16. Fahmy K, Jager F, Beck M, Zvyaga TA, Sakmar TP, Siebert F (1993) Proc Natl Acad Sci USA 90:10206–10210
17. Ferré N, Olivucci M (2003) J Am Chem Soc 125:6868–6869
18. Singh UC, Kollman PA (1986) J Comp Chem 7:718–730
19. Ferré N, Olivucci M (2003) Theochem 632:71–82
20. Ferré N, Cembran A, Garavelli M, Olivucci M (2004) Theor Chem Acc 112:335–341
21. Gaussian 03 RC, Frisch MJ, Trucks GW, Schlegel HB, Scuseria GE, Robb MA, Cheeseman JR, Montgomery JA, Jr, Vreven T, Kudin KN, Burant JC, Millam JM, Iyengar SS, Tomasi J, Barone V, Mennucci B, Cossi M, Scalmani G, Rega N, Petersson GA, Nakatsuji H, Hada M, Ehara M, Toyota K, Fukuda R, Hasegawa J, Ishida M, Nakajima T, Honda Y, Kitao O, Nakai H, Klene M, Li X, Knox JE, Hratchian HP, Cross JB, Bakken V, Adamo C, Jaramillo J, Gomperts R, Stratmann RE, Yazyev O, Austin AJ, Cammi R, Pomelli C, Ochterski JW, Ayala PY, Morokuma K, Voth GA, Salvador P, Dannenberg JJ, Zakrzewski VG, Dapprich S, Daniels AD, Strain MC, Farkas O, Malick DK, Rabuck AD, Raghavachari K, Foresman JB, Ortiz JV, Cui Q, Baboul AG, Clifford S, Cioslowski J, Stefanov BB, Liu G, Liashenko A, Piskorz P, Komaromi I, Martin RL, Fox DJ, Keith T, Al-Laham MA, Peng CY, Nanayakkara A, Challacombe M, Gill PMW, Johnson B, Chen W, Wong MW, Gonzalez C, Pople JA (2004) Gaussian, Inc, Wallingford CT
22. Ponder JW, Richards FM (1987) J Comp Chem 8:1016–1024
23. Sugihara M, Buss V, Entel P, Hafner J (2004) J Phys Chem B 108:3673–3680
24. Hufen J, Sugihara M, Buss V (2004) J Phys Chem B 108:20419–20426
25. Cembran A, Bernardi F, Olivucci M, Garavelli M (2005) Proc Nat Acad Sci USA 102:6255–6260
26. Bonacic-Koutecky V, Köhler K, Michl J(1984) Chem Phys Lett 104:440–443
27. Bonacic-Koutecky V, Schöffel KJ, Michl J (1987) Theor Chim Acta 72:459–474
28. Birge RR, Murray LP, Pierce BM, Akita H, Balogh-Nair V, Findsen LA, Nakanishi K (1985) Proc Natl Acad Sci USA 82:4117–4121